Bioorganic Chemistry 81 (2018) 134–143

Contents lists available at ScienceDirect

Bioorganic Chemistry

journal homepage: www.elsevier.com/locate/bioorg

Short communication

Highly functionalized 2-amino-4*H*-pyrans as potent cholinesterase inhibitors

Raju Suresh Kumar[a,*], Abdulrahman I. Almansour[a], Natarajan Arumugam[a], Dhaifallah M. Al-thamili[a], Alireza Basiri[b], D. Kotresha[c], Thota Sai Manohar[d], S. Venketesh[d], Mohammad Asad[e,f], Abdullah M. Asiri[e,f]

[a] Department of Chemistry, College of Sciences, King Saud University, P.O. Box 2455, Riyadh 11451, Saudi Arabia
[b] Department of Pharmaceutical Sciences, College of Pharmacy, University of Nebraska Medical Center, Omaha, NE 68198, United States
[c] Department of Microbiology, East West Group of Institution, no. 63, Anjananagar, Vishwaneedam post, Bangaluru 560091, Karnataka, India
[d] Department of Biosciences, Sri Sathya Sai Institute of Higher Learning, Prasanthi Nilayam, A.P. 515 134, India
[e] Chemistry Department, Faculty of Science, King Abdulaziz University, Jeddah 21589, Saudi Arabia
[f] Center of Excellence for Advanced Materials Research (CEAMR), King Abdulaziz University, Jeddah 21589, Saudi Arabia

ARTICLE INFO

Keywords:
2-amino-4*H*-pyrans
Alzheimer's disease
AChE
BChE
Molecular docking simulations

ABSTRACT

Novel highly functionalized 2-amino-4*H*-pyrans were achieved in excellent yields under simple grinding at ambient temperature and were assessed for their potential for treating Alzheimer's disease (AD). The 2-amino-4*H*-pyran bearing nitro groups on both the aryl rings showed the highest activity, with an IC_{50} of 1.98 ± 0.09 μM against acetylcholinesterase (AChE) and 10.62 ± 0.21 μM against butyrylcholinesterase (BChE), the inhibition mechanisms on AChE and BChE receptors were revealed by means of molecular docking simulations.

1. Introduction

Most of the developed countries will experience a intense demographic shift toward an older population in the next 50 years, which is expected to significantly rise the occurrence of Alzheimer's disease (AD), the increase in the number of AD patients will place an excessive social and economic encumbrance on the developed world [1]. AD is an age-allied neurodegenerative disease categorized clinically by a progressive drop in memory and language [2] and pathologically by accumulation of senile plaques and neurofibrillary tangles in the brain [3]. AD is represented with characteristic symptoms, i.e. changes in levels of cholinesterase (ChEs), enhanced production and accumulation of β-amyloid peptide, formation of neurofibrillary tangles inside nerve cell bodies etc. In process of development of AD, the levels of ChEs are altered in different manner. In early stages of AD, the level of AChE is increased at a much higher rate than BChE while in later stages, level of AChE decreases and rapid increase in BChE level occurs in brain. In this stage, BChE substitutes the function of AChE – the hydrolysis of acetylcholine (ACh). Generally, the lower level of ACh during AD is obvious and therefore inhibition of ChEs represents one of the major pharmacological interventions for this disease [4] and hence ChE inhibitors are widely used to rectify cholinergic transmission in the treatment of AD.

As in the current scenario most of therapeutic treatments for AD has focused on the inhibition of ChEs [5], the discovery of new cholinesterase inhibitors that can become new drug candidates for the treatment of AD is still a goal for the scientific community and is the purpose of this work. It is pertinent to note that for the last few years, we have been involved in the discovery of novel organic molecules as ChE inhibitors [6–15]. Under this context, we would like to explore the possibility of functionalized pyran derivatives designed and synthesized by us as ChE inhibitors.

Pyran derivatives, the most honored heterocyclic frameworks occupy a significant place in the realm of natural and synthetic organic chemistry due to their simple structural complexity and important biological activities [16–22]. Among the pyrans, 4*H*-pyran-annulated heterocyclic frameworks are well distributed in naturally occurring compounds [23–25] and demonstrates a widespread array of biological activities such as antitumor, antibacterial, antiviral, spasmolytic, and anti-anaphylactic [26–29]. Compounds possessing 4*H*-pyran core structure have also been established in treating AD, schizophrenia, and Myoclonus disease [30]. It is worthy to mention that currently, a number of drug molecules bearing 4*H*-pyran moiety are in use in the treatment of various diseases [31–35]. Fig. 1 represents some of the pyran-annulated heterocyclic compounds exhibiting diverse kind of pharmaceutical applications [36–40]. In view of the biological significance of these functionalized pyrans in medicinal chemistry and also

* Corresponding author.
E-mail address: sraju@ksu.edu.sa (R.S. Kumar).

https://doi.org/10.1016/j.bioorg.2018.08.009
Received 20 May 2018; Received in revised form 5 August 2018; Accepted 7 August 2018
Available online 12 August 2018

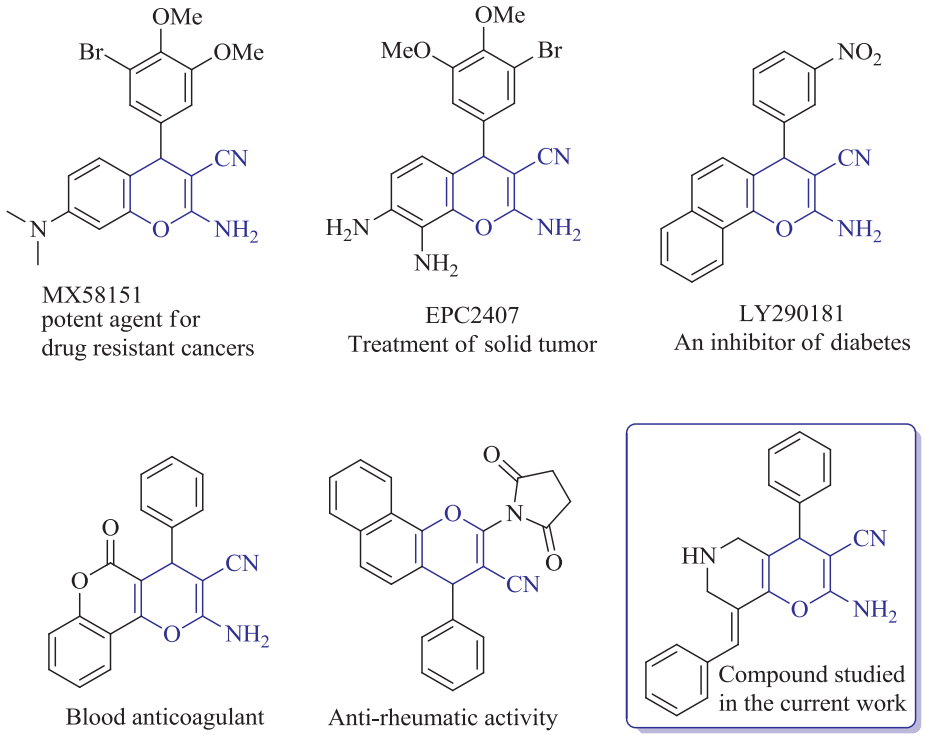

Fig. 1. Some of the biologically and pharmacologically active 4*H*-pyrans.

due to the fact that there have been less reports for 2-amino-4*H*-pyran derivatives as cholinesterase inhibitors [41], herein we aimed to explore our preliminary findings on the green synthesis and anticholinesterase activity of functionalized 4*H*-pyran derivatives.

2. Results and discussion

2.1. Chemistry

Schematic representation for the synthesis of desired 2-amino-4*H*-pyran derivatives **4(a-n)** is demonstrated in Scheme 1. The starting precursors *viz*, 3,5-bis[(*E*)-*arylmethylidene*]tetrahydro-4(1*H*)-pyridinones **2(a-n)** were synthesized following the method reported by dimmock et al. [42]. With a small library of these bisarylidenepyridinone derivatives in hand, we then performed the reaction of **2** with malononitrile (**3**). In a representative experiment, an equimolar mixture of **2i**, **3** and solid sodium ethoxide at ambient temperature was milled thoroughly for 2–3 min. Completion of the reaction was designated by the fading color of the reaction mixture, which became colorless at the end of the reaction, thus avoiding TLC monitoring. It is pertinent to note that the product **4i** was obtained in excellent yield (96%). As this reaction affords solely 2-amino-4*H*-pyrans **4(a–n)** without any impurities, purification of the products involving either crystallization or column chromatography is not required. All of the 2-amino-*4*H-pyran derivatives **4(a–n)** were obtained in quantitative yields, except for the slight loss during workup. All the fourteen 2-amino-4*H*-pyran derivatives synthesized are new and their structures are in good agreement with their spectroscopic data. Scaling up of the reaction does not envisage any drop in either the yield or purity of the product, as the reaction requires only a thorough mixing of the reactants at ambient temperature, which can be readily confirmed by suitable grinds. The easy availability of starting precursors, short reaction time and high yield of the products renders this method more attractive.

The structure of **4** was elucidated using FT-IR, NMR spectroscopic and Mass spectrometry studies considering **4i** as a representative case (vide supplementary data).

Supplementary data associated with this article can be found, in the online version, at https://doi.org/10.1016/j.bioorg.2018.08.009.

The mechanism depicted in Scheme 2 envisages an initial Michael addition of the active methylene compound malanonitrile (**3**) to α,β-unsaturated moiety of **2** to afford the Michael adduct **5** which upon tautomerisation affords compound **6**. Cyclisation of **6** leads to the

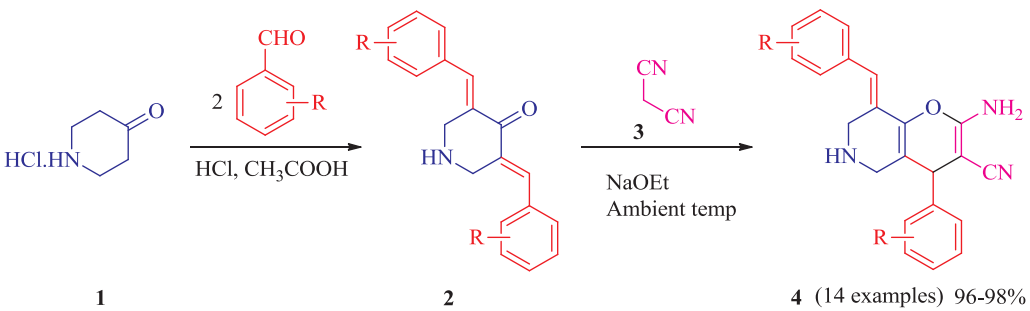

Scheme 1. Synthesis of highly functionalized 2-amino-4*H*-pyrans **(4a-n)**.

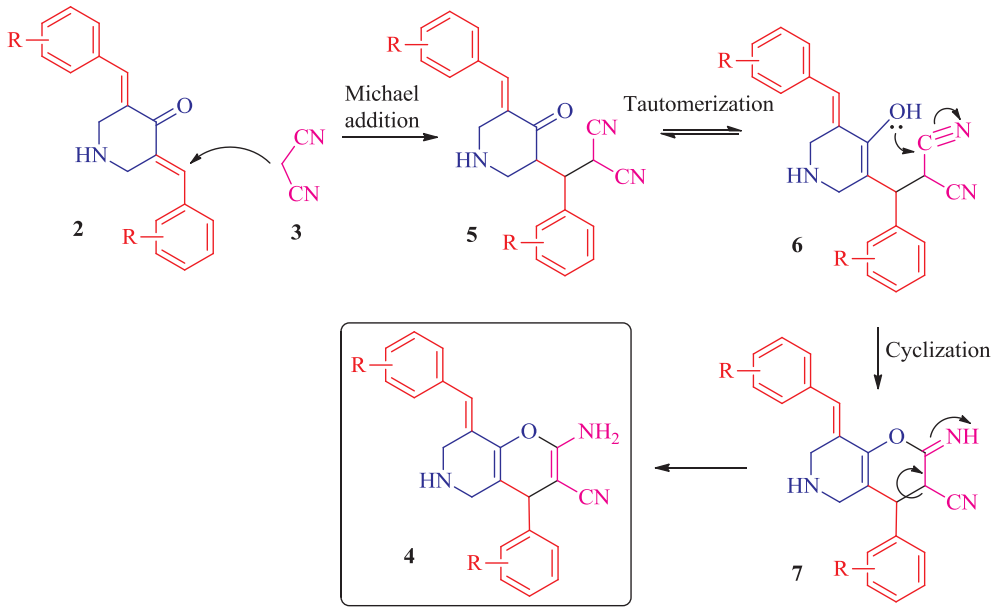

Scheme 2. Plausible mechanism for the formation of 2-amino-4*H*-pyrans **4**.

formation of the highly functionalized pyrans, *viz.* 2-amino-4-aryl-8-[(*E*)-arylmethylidene]-5,6,7,8-tetrahydro-4*H*-pyrano[3,2-*c*]pyridin-3-carbonitriles **4** via the intermediate **7**.

2.2. Biochemistry

2.2.1. Cholinesterase inhibitory analysis

All new 2-amino-4*H*-pyrans **4(a-n)** synthesized in the present study were assessed *in vitro* for their activity against AChE and BChE enzymes and the results are summarized in table 1. For AChE, all the compounds showed significant activity with IC_{50} 1.98 ± 0.09–21.20 ± 0.15 μM. It is evident from Table 1 that the compound **4h**, bearing the nitro groups on aryl rings, displayed the highest AChE inhibitory activity with an IC_{50} value of 1.98 ± 0.09 μM followed by compound **4i**, bearing methyl group on the aryl ring with IC_{50} value of 2.44 ± 0.16 μM. These two leads showed better or comparable activity to the standard drug, galanthamine, with IC_{50} value of 2.09 ± 0.13 μM. This may lead to better insertion and accommodation of the inhibitor(s) inside the active site of the AChE enzyme. Compounds **4a**, **4b**, **4j** and **4m** with H, 2-Me, 4-OMe and 4-F groups respectively also showed good activities with IC_{50} less than 10 μM. Other compounds **4c-g**, **4k**, **4l** and **4n** with 2-OMe, 2-Cl, 2-Br, 2-F, 2,4-Cl_2, 4-Cl, 4-Br and naphthyl substituents showed moderate activity when compared to the standard drug Galantamine. For AChE, no clear trend has been observed on how the activities differ with respect to the electronic nature of the attached functional groups.

Table 1
AChE and BChE inhibitory activities of 2-amino-4*H*-pyrans **4(a-n)**.

Entry	Comp	AChE Inhibition IC_{50} μM (± SD)	BChE inhibition IC_{50} μM (± SD)	Selectivity	
				AChE[a]	BChE[b]
1	**4a**: R = C_6H_5	5.98 ± 0.15	14.63 ± 0.24	2.45	0.41
2	**4b**: R = 2-$CH_3C_6H_4$	6.85 ± 0.07	12.40 ± 0.14	1.81	0.55
3	**4c**: R = 2-$OCH_3C_6H_4$	10.51 ± 0.18	16.70 ± 0.25	1.59	0.63
4	**4d**: R = 2-ClC_6H_4	18.20 ± 0.15	13.47 ± 0.12	0.74	1.35
5	**4e**: R = 2-BrC_6H_4	16.36 ± 0.23	20.61 ± 0.14	1.26	0.81
6	**4f**: R = 2-FC_6H_4	12.54 ± 0.25	18.74 ± 0.10	1.49	0.67
7	**4g**: R = 2,4-$Cl_2C_6H_3$	21.20 ± 0.15	14.53 ± 0.12	0.69	1.46
8	**4h**: R = 3-$NO_2C_6H_4$	1.98 ± 0.09	10.62 ± 0.21	5.36	0.19
9	**4i**: R = 4-$CH_3C_6H_4$	2.44 ± 0.16	12.75 ± 0.18	5.23	0.19
10	**4j**: R = 4-$OCH_3C_6H_4$	7.38 ± 0.15	26.68 ± 0.22	3.62	0.28
11	**4k**: R = 4-ClC_6H_4	10.22 ± 0.16	23.15 ± 0.12	2.27	0.44
12	**4l**: R = 4-BrC_6H_4	13.64 ± 0.16	19.77 ± 0.25	1.45	0.69
13	**4m**: R = 4-FC_6H_4	8.51 ± 0.21	24.81 ± 0.14	2.92	0.34
14	**4n**: R = $C_{10}H_7$	15.40 ± 0.20	17.15 ± 0.08	1.11	0.90
15	Galantamine	2.09 ± 0.13	19.34 ± 0.18	9.25	0.11

[a] Selectivity for AChE defined as IC_{50}(BChE)/IC_{50}(AChE).
[b] Selectivity for BChE defined as IC_{50}(AChE)/IC_{50}(BChE).

Similarly, for BChE all these 2-amino-4*H*-pyrans **4(a-n)** displayed good inhibitory activities with IC_{50} values ranging from 10.62 ± 0.21–26.68 ± 0.22 μM. All the compounds except **4e**, **4j**, **4k** and **4m** showed almost similar or higher BChE activities than the standard drug galanthamine (19.34 ± 0.18 μM), compound **4h** again being the most potent inhibitor compared to other members of the series. These results discovered that the existence of nitro group on the aryl ring, had significant effect on the inhibitory activities, these results has also been supported from our recent study [43] wherein compounds bearing nitro group displayed the highest cholinesterase inhibitory activity.

It can be concluded that these series of compounds are active against both AChE and BChE enzymes. It is evident from Table 2 that a good selectivity has been observed toward AChE than BChE. Hence, compound **4h** can be considered as a "hit" that can be modified to improve its potencies against ChE enzymes.

2.2.2. Molecular docking

AutoDock/Vina plugin is used to evaluate the docking of the two most active compounds, **4h** and **4i**, with hAChE and hBChE receptors. The binding affinity of the compounds is good toward both the receptors, however, the affinity of the ligand **4h** is better (binding energy of −11.0 kcal/mol with hAChE and −10.6 kcal/mol with hBChE) when compared to ligand **4i**. Table 2 and Figs. 2–5 summarizes the amino acids of hACHE and hBCHE involved in the interactions (H-bonding and hydrophobic) with the ligands. The affinity of **4h** toward hAChE and hBChE is stronger than **4i** due to the H-bondings of "3-$NO_2C_6H_4$" group. To understand the role of "R" groups on the ligands **4h** and **4i**, docking is done with the unsubstituted ligand **4a** and the binding energies and interacting amino acids are compared with that of ligands **4h** and **4i** and summarized in Table 2. We observed that the binding affinity of **4a** has reduced slightly in comparison to **4h**, whereas this trend is not observed for **4i**. The interactions of "R" group in **4h** and **4i** with the

Table 2
Amino acid residues involved in H-bonding and hydrophobic interactions with ligands.

Comp	Enzyme	Binding Energy (kcal/mol)	Interacting amino acids
4a	hAChE	−10.7	**Hydrophobic interaction:** Asp74, Gly121, Gly122, Tyr124, Ser125, Trp286, Val294, Phe295, Phe297, Phe338, Tyr341, Tyr449 **H-bonding:** Trp86, Tyr337
	hBChE	−10.1	**Hydrophobic interaction:** Asn68, Ile69, Asp70, Gly116, His438 **H-bonding:** Trp82, Gly115, Thr120, Tyr128
4h	hAChE	−11.0	**Hydrophobic interaction:** Asp74, Gly121, Gly122, Tyr124, Ser125, Trp286, Val294, Phe295, Phe297, Phe338, Tyr341, Tyr449 **H-bonding:** Trp86, Tyr337, His447
	hBChE	−10.6	**Hydrophobic interaction:** Asp70, Trp82, Glu197, Phe329, Tyr332, Tyr440 **H-bonding:** Gly116, Gly117, Thr120, Ser198, His438
4i	hAChE	−9.3	**Hydrophobic interaction:** Gly120, Gly121, Gly122, Tyr124, Ser125, Glu202, Trp286, Ser293, Val294, Phe297, Tyr337, Phe338, Tyr341, Gly448, Ile451 **H-bonding:** Trp86
	hBChE	−10.2	**Hydrophobic interaction:** Asn68, Ile69, Asp70, Gly115, Gly116, His438, Tyr440 **H-bonding:** Trp82, Thr120, Tyr128

receptors are provided in supplementary data (Figs. S8–S11).

Ligand **4h** formed three H-bonds with hAChE; Trp86 (bond length: 3.07), Tyr337 (bond length: 3.33), His447 (bond length: 3.28) and formed six H-bonds with hBChE; Two with Ser198 (bond length: 3.02 and 3.29) and one each with Gly116 (bond length:3.22), Gly117 (bond length:2.88), Thr120 (bond length:3.23), His438 (bond length:3.10). Ligand **4i** formed one H-bond with Trp86 (bond length: 2.95) of hAChE and three H-bonds with hBChE; Trp82 (bond length: 2.84), Thr120 (bond length: 2.93) Tyr 128 (bond length: 3.01). The selectivity of the ligands, **4h** and **4i**, is better toward hAChE than toward hBChE, which can be seen with the increased number of hydrophobic interactions with hAChE.

Fig. 6 (surface view) and Fig. 7 (cartoon view) shows the docking of **4h** with the active site of hAChE and hBChE.

For a molecule to be a potent drug, it should be assessed for absorption, distribution, metabolism and excretion (ADME). Using the Swiss ADME web tool [44] (http://www.swissadme.ch), we calculated physicochemical properties, lipophilicity, water solubility, pharmacokinetics, drug-likeness and medicinal chemistry friendliness of compounds **4h** and **4i** and are summarized in Table 3.

According to Brain Or IntestinaL EstimateD permeation method [45] (BOILED-egg), compound **4i** is passively permeated by the blood-brain barrier (BBB) and also absorbed by the gastrointestinal (GI) tract whereas compound **4h** is not. Both the compounds are predicted to be effluated from the central nervous system by the P-glycoprotein. Fig. 8 shows the compounds **4h** and **4i** mapped onto the BOILED-Egg.

Potential targets of compounds **4h** and **4i** are computationally predicted using the molecular structural similarity and molecular shape using the Swiss Target Prediction [50]. The predicted target classes have been summarized in Fig. 9 using a pie chart. The ligand **4h** has higher affinity than **4i** toward transporter class, whereas the ligand **4i** has affinity toward transcription factors while this factor is absent in **4h**.

3. Conclusion

We described the synthesis of a small library of 2-amino-4H-pyrans **4(a-n)**, the method employed is far more advantageous than the

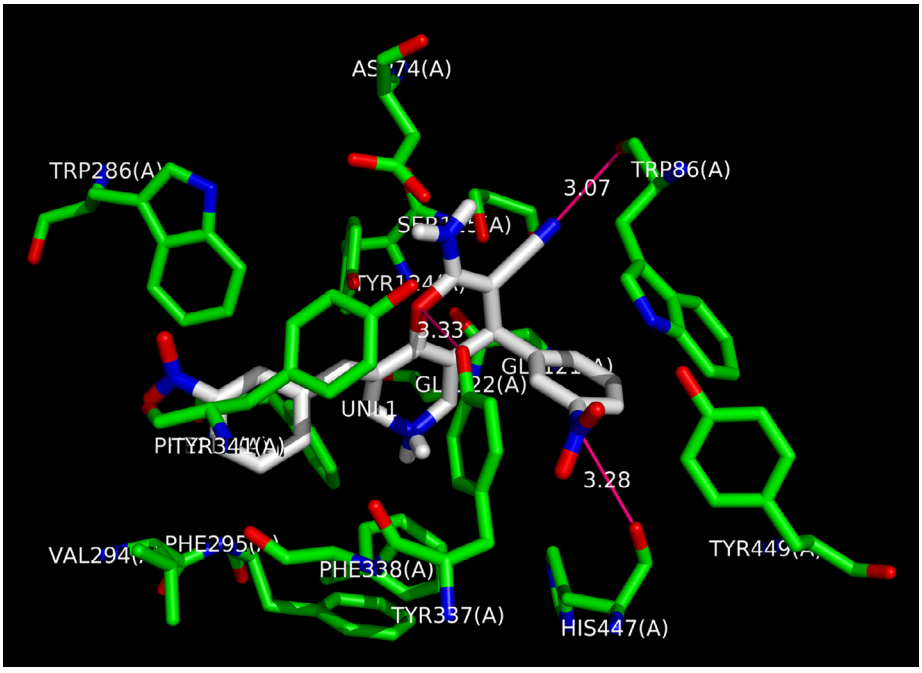

Fig. 2. Ligand **4h** interacting with hAChE. Shown in green are the binding site amino acids involved in the interactions.

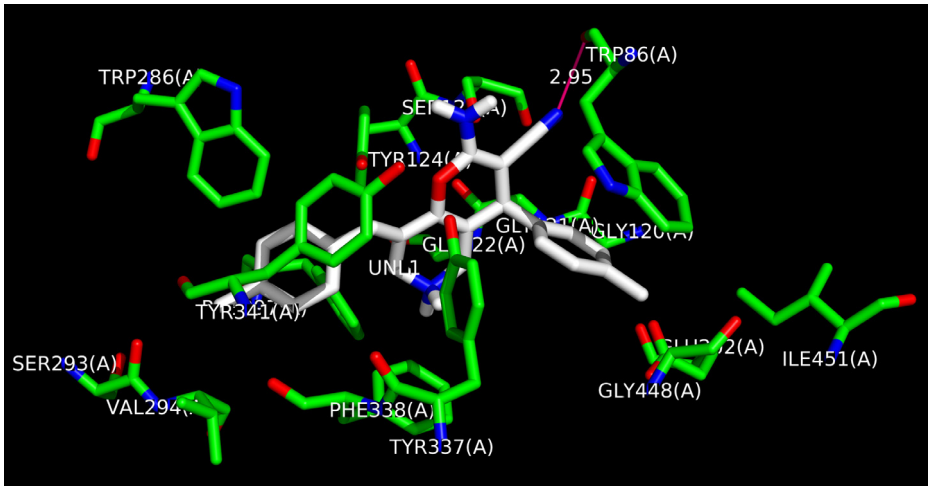

Fig. 3. Ligand **4h** interacting with hBChE. Shown in green are the binding site amino acids involved in the interactions.

literature reported procedures for the synthesis of 4H-pyrans with respect to time, eco-friendliness and yield. The easy obtainability of the reagents and short reaction time renders this method more attractive. Furthermore, these derivatives **4**(**a-n**) were assayed for their inhibitory potential against AChE and BChE. Compound **4h** with nitro group on the aryl ring displayed the highest inhibitory activity with an IC50 of 1.98 ± 0.09 μM against AChE and 10.62 ± 0.21 μM against BChE. The docking study also showed that these compounds had the potential to dock and bind with both AChE and BChE. Hence, compound **4h** can be considered as a "hit" with diverse functionalities such as NH, NH2 and nitrile groups which paves the way for further modifications that can improve its potencies against ChE enzymes.

4. Experimental

4.1. General procedure for the synthesis of 2-amino-4H-pyrans *4(a-n)*

In a typical experiment, an equimolar mixture of 2 and malononitrile with a catalytic amount of sodium ethoxide was milled thoroughly at room temperature. The reaction progress is specified by the fading color of the reaction mixture, which became colorless at the end of the reaction. Addition of 50 mL of ice cold water to the reaction mixture furnished the precipitate which then was filtered to afford the pure product.

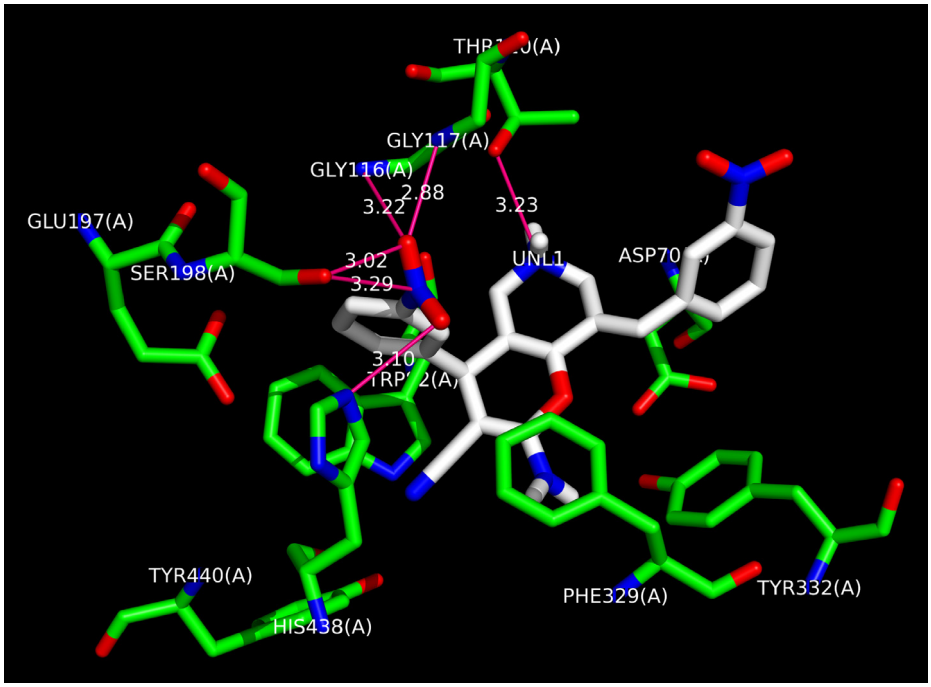

Fig. 4. Ligand **4i** interacting with hAChE. Shown in green are the binding site amino acids involved in the interactions.

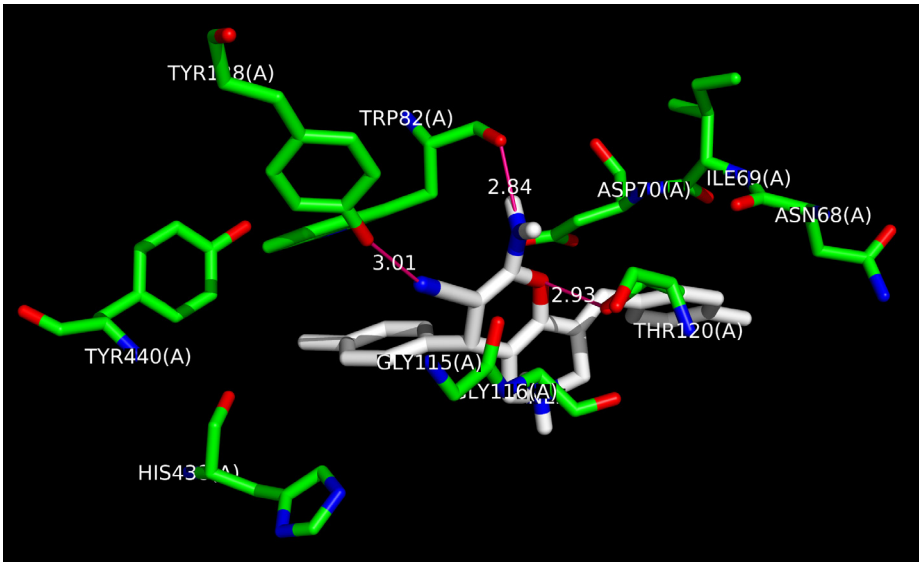

Fig. 5. Ligand **4i** interacting with hBChE. Shown in green are the binding site amino acids involved in the interactions.

4.2. Characterization data for compound *4a*

White solid, 98% (0.122 g), mp 170–172 °C, IR (KBr)υ_{max} 3389, 2177, 1678, 1601 cm^{-1}; ^1H NMR (400 MHz, $CDCl_3$): δ_H 3.16 (1H, d, J = 17.2 Hz), 3.29 (1H, d, J = 17.2 Hz), 3.80 (1H, dd, J = 15.2, 1.6 Hz), 3.92 (1H, dd, J = 15.2, 1.2 Hz), 4.00 (1H, s), 4.59 (2H, s), 6.86 (1H, s), 7.21–7.31 (7H, m), 7.33–7.36 (3H, m); ^{13}C NMR (100 MHz, $CDCl_3$): δ_C 41.6, 45.9, 46.5, 58.8, 114.6, 120.3, 122.0, 127.1, 127.4, 127.8, 128.3, 128.6, 128.8, 129.1, 130.4, 136.3, 142.8, 159.7. LC/MS (ESI): 342 (M^+). Anal. calcd for $C_{22}H_{19}N_3O$: C, 77.40; H, 5.61; N, 12.31%; found: C, 77.58; H, 5.72; N, 12.23%.

4.3. Characterization data for compound *4b*

White solid, 97% (0.118 g), mp 120–124 °C, IR (KBr)υ_{max} 3372, 2177, 1642, 1598 cm^{-1}; ^1H NMR (400 MHz, $CDCl_3$): δ_H 2.34 (3H, s), 2.44 (3H, s), 3.10 (1H, d, J = 17.2 Hz), 3.26 (1H, d, J = 17.2 Hz), 3.66 (1H, d, J = 16.0 Hz), 3.75 (1H, d, J = 16.0 Hz), 4.38 (1H, s), 4.69 (2H, s), 6.88 (1H, s), 7.06–7.25 (8H, m); ^{13}C NMR (100 MHz, $CDCl_3$): δ_C 19.9, 20.5, 37.5, 46.4, 46.9, 60.5, 115.1, 120.3, 121.5, 125.9, 127.3, 127.7, 127.8, 128.0, 129.1, 129.5, 130.5, 131.3, 135.5, 136.1, 137.2, 140.7, 140.9, 159.4. LC/MS (ESI): 369 (M^+). Anal. calcd for $C_{24}H_{23}N_3O$: C, 78.02; H, 6.27; N, 11.37%; found: C, 78.25; H, 6.11; N, 11.45%.

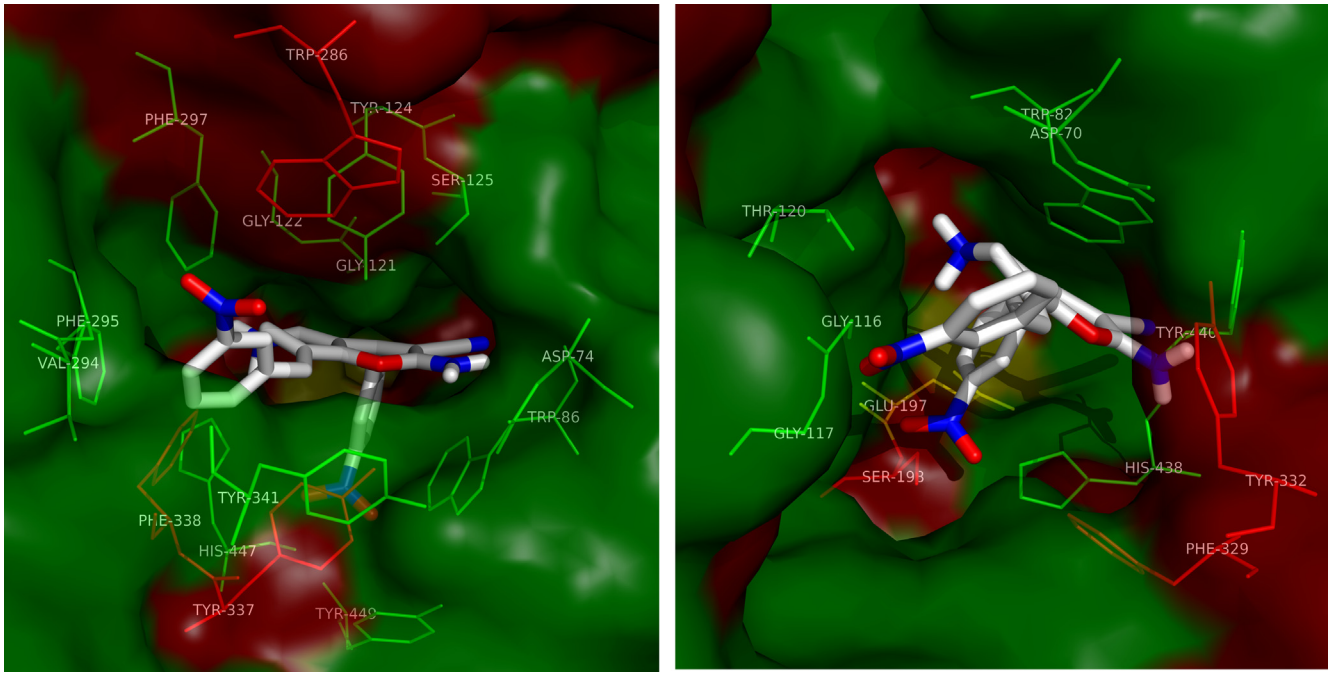

Fig. 6. Active site (surface view) of (A) hAChE and (B) hBChE docked with ligand **4h** (stick view). Amino acids involved in the interactions are represented as lines.

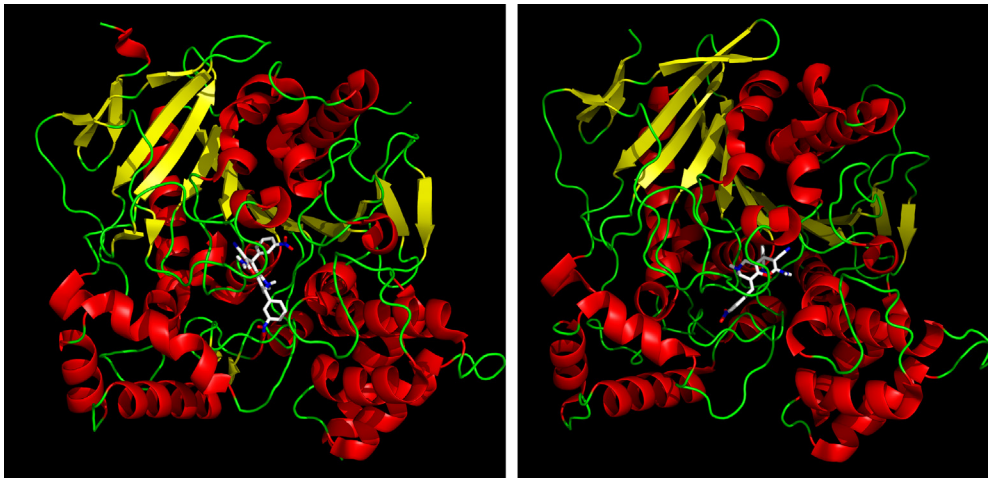

Fig. 7. Cartoon view of (A) hAChE and (B) hBChE docked with ligand **4h.**

4.4. Characterization data for compound **4c**

Yellow solid, 92% (0.110 g), mp 156–158 °C, IR (KBr)υ_{max} 3320, 2182, 1630, 1597 cm^{-1}; ^1H NMR (300 MHz, $CDCl_3$): δ_H 3.16 (1H, d, J = 17.4 Hz), 3.35 (1H, d, J = 17.4 Hz), 3.70 (1H, d, J = 16.2 Hz), 3.80 (1H, d, J = 16.2 Hz), 3.84 (3H, s), 3.86 (3H, s), 4.62–4.64 (3H, m), 6.87–7.29 (9H, m); ^{13}C NMR (75 MHz, $CDCl_3$): δ_C 38.3, 46.6, 46.8, 55.8, 56.0, 60.2, 110.8, 111.3, 115.5, 117.7, 120.5, 120.6, 121.6, 125.4, 128.1, 128.9, 129.3, 129.4, 130.7, 131.0, 141.1, 157.4, 157.6, 160.2. LC/MS (ESI): 401 (M^+). Anal. calcd for $C_{24}H_{23}N_3O_3$: C, 71.80; H, 5.77; N, 10.47%; found: C, 71.63; H, 5.90; N, 10.58%.

4.5. Characterization data for compound **4d**

White solid, 96% (0.115 g), mp 200–202 °C, IR (KBr)υ_{max} 3365, 2177, 1642, 1598 cm^{-1}; ^1H NMR (400 MHz, $CDCl_3$): δ_H 3.03 (1H, d, J = 17.2 Hz), 3.31 (1H, d, J = 17.6 Hz), 3.57 (1H, d, J = 15.2 Hz), 3.68 (1H, d, J = 15.2 Hz), 4.64 (1H, s), 5.26 (2H, s), 6.88 (1H, s), 7.07–7.36 (8H, m); ^{13}C NMR (100 MHz, $CDCl_3$): δ_C 37.8, 46.2, 46.5, 58.4, 115.4, 119.7, 120.2, 126.8, 128.1, 129.1, 129.2, 129.9, 130.1, 130.7, 131.0, 133.7, 134.2, 134.7, 140.1, 140.7, 160.3. LC/MS (ESI): 411 (M^+). Anal. calcd for $C_{22}H_{17}Cl_2N_3O$: C, 64.40; H, 4.18; N, 10.24%; found: C, 64.55; H, 4.30; N, 10.36%.

4.6. Characterization data for compound **4e**

White solid, 94% (0.108 g), mp 184–186 °C, IR (KBr)υ_{max} 3362, 2179, 1645, 1599 cm^{-1}; ^1H NMR (300 MHz, $CDCl_3$): δ_H 3.10 (1H, d, J = 17.4 Hz), 3.40 (1H, d, J = 17.4 Hz), 3.64 (1H, d, J = 15.6 Hz), 3.75 (1H, d, J = 15.6 Hz), 4.75 (3H, s), 6.87 (1H, s), 7.11–7.38 (6H, m), 7.55 (1H, d, J = 7.8 Hz), 7.61 (1H, d, J = 7.8 Hz); ^{13}C NMR (75 MHz, $CDCl_3$): δ_C 40.3, 46.3, 46.6, 59.8, 115.7, 119.7, 122.2, 124.1, 124.8, 127.5, 128.8, 129.4, 129.6, 131.0, 133.3, 133.6, 136.5, 140.7, 159.8. LC/MS (ESI): 499 (M^+). Anal. calcd for $C_{22}H_{17}Br_2N_3O$: C, 52.93; H, 3.43; N, 8.42%; found: C, 52.75; H, 3.59; N, 8.54%.

4.7. Characterization data for compound **4f**

White solid, 95% (0.115 g), mp 174–176 °C, IR (KBr)υ_{max} 3331, 2180, 1627, 1600 cm^{-1}; ^1H NMR (300 MHz, $CDCl_3$): δ_H 3.18 (1H, d, J = 17.4 Hz), 3.37 (1H, d, J = 17.4 Hz), 3.67 (1H, d, J = 15.0 Hz), 3.80 (1H, d, J = 15.0 Hz), 4.45 (1H, s), 4.74 (2H, s), 6.84 (1H, s), 7.03–7.40 (8H, m); ^{13}C NMR (75 MHz, $CDCl_3$): δ_C 34.4, 46.5, 46.7, 59.1, 115.9, 116.2, 119.9, 124.2, 124.3, 124.4, 125.3, 129.2, 129.6, 129.7, 130.2, 130.9, 131.3, 137.1, 140.9, 160.1, 162.2, 162.6. LC/MS (ESI): 377 (M^+). Anal. calcd for $C_{22}H_{17}F_2N_3O$: C, 70.02; H, 4.54; N, 11.13%; found: C, 70.25; H, 4.39; N, 11.01%.

4.8. Characterization data for compound **4g**

Pale yellow solid, 96% (0.110 g), mp 132–135 °C, IR (KBr)υ_{max} 3313, 2184, 1635, 1601 cm^{-1}; ^1H NMR (400 MHz, $CDCl_3$): δ_H 3.11 (1H, d, J = 17.6 Hz), 3.39 (1H, d, J = 17.6 Hz), 3.64 (1H, d, J = 15.2 Hz), 3.74 (1H, d, J = 15.2 Hz), 4.69 (1H, s), 4.82 (2H, s), 6.86 (1H, s), 7.08 (1H, d, J = 8.0 Hz), 7.24–7.46 (5H, m); ^{13}C NMR (100 MHz, $CDCl_3$): δ_C 37.5, 46.2, 46.5, 59.4, 115.4, 119.0, 119.5, 127.2, 128.6, 129.5, 130.0, 130.1, 131.5, 131.6, 132.5, 133.1, 134.3, 134.4, 135.1, 138.4, 140.9, 159.9. LC/MS (ESI): 479 (M^+). Anal. calcd for $C_{22}H_{15}Cl_4N_3O$: C, 55.14; H, 3.16; N, 8.77%; found: C, 55.40; H, 3.38; N, 8.65%.

4.9. Characterization data for compound **4h**

Orange solid, 97% (0.115 g), mp 168–170 °C, IR (KBr)υ_{max} 3343, 2184, 1635, 1598 cm^{-1}; ^1H NMR (400 MHz, $CDCl_3$): δ_H 3.10 (1H, d, J = 17.2 Hz), 3.35 (1H, d, J = 17.6 Hz), 3.79 (1H, d, J = 15.2 Hz), 3.92 (1H, d, J = 15.2 Hz), 4.21 (1H, s), 6.24 (2H, s), 7.04 (1H, s), 7.57–7.68 (4H, m), 8.08–8.15 (4H, m); ^{13}C NMR (100 MHz, $CDCl_3$): δ_C 41.0, 45.1, 45.6, 56.9, 114.3, 119.5, 121.2, 122.0, 123.1, 123.9, 129.0, 129.4, 129.6, 133.7, 134.4, 137.5, 139.9, 144.7, 147.6, 148.0, 159.5. LC/MS (ESI): 431 (M^+). Anal. calcd for $C_{22}H_{17}N_5O_5$: C, 61.25; H, 3.97; N, 16.23%; found: C, 61.43; H, 3.85; N, 16.31%.

4.10. Characterization data for compound **4i**

Yellow solid, 96% (0.117 g), mp 118–121 °C, IR (KBr)υ_{max} 3321, 2184, 1635, 1594 cm^{-1}; ^1H NMR (400 MHz, $CDCl_3$): δ_H 2.32 (3H, s), 2.35 (3H, s), 3.14 (1H, d, J = 17.2 Hz), 3.24 (1H, d, J = 17.2 Hz), 3.77 (1H, d, J = 15.2 Hz), 3.88–3.93 (2H, m), 4.71 (2H, s), 6.81 (1H, s), 7.10–7.17 (8H, m); ^{13}C NMR (100 MHz, $CDCl_3$): δ_C 21.5, 21.7, 41.4, 46.4, 46.8, 60.8, 114.8, 120.4, 122.5, 127.2, 128.1, 129.5, 129.6, 130.0, 133.7, 137.6, 137.7, 139.8, 140.7, 159.4. LC/MS (ESI): 369 (M^+). Anal. calcd for $C_{24}H_{23}N_3O$: C, 78.02; H, 6.27; N, 11.37%; found: C, 78.29; H, 6.40; N, 11.48%.

4.11. Characterization data for compound **4j**

Yellow solid, 95% (0.114 g), mp 133–135 °C, IR (KBr)υ_{max} 3332, 2186, 1628, 1598 cm^{-1}; ^1H NMR (300 MHz, $CDCl_3$): δ_H 3.14 (1H, d, J = 17.4 Hz), 3.36 (1H, d, J = 17.4 Hz), 3.73 (1H, d, J = 16.2 Hz), 3.82 (1H, d, J = 16.2 Hz), 3.86 (3H, s), 3.88 (3H, s), 4.65–4.67 (3H, m),

Table 3
Illustrates some of the important properties of compounds **4h** and **4i** using SwissADME web tools.

Properties	4h	4i
Physicochemical properties		
Formula	C22H17N5O5	C24H23N3O
Molecular weight	431.40 g/mol	369.46 g/mol
Num. rotatable bonds	4	2
Num. H-bond acceptors	7	3
Num. H-bond donors	2	2
Molar Refractivity	122.20	114.49
*TPSA	162.71 Å^2	71.07 Å^2
Lipophilicity		
Log *P* (average of iLOGP, XLOGP3, WLOGP, MLOGP, SILICOS-IT)	1.34	3.50
Water solubility		
#Log *S* (ESOL)	−3.93	−4.39
Solubility	5.11e−02 mg/ml; 1.18e−04 mol/l	1.51e−02 mg/ml; 4.09e−05 mol/l
Class	Soluble	Moderately soluble
Pharmacokinetics		
GI absorption	Low	High
BBB permeant	No	Yes
P-gp substrate	Yes	Yes
CYP1A2 inhibitor	No	Yes
CYP2C19 inhibitor	No	Yes
CYP2C9 inhibitor	Yes	Yes
CYP2D6 inhibitor	No	No
CYP3A4 inhibitor	Yes	Yes
$Log K_p (skin permeation)	−7.36 cm/s	−6.22 cm/s
Druglikeness		
Lipinski (Pfizer) filter	Yes; 0 violation	Yes; 0 violation
Ghose filter	Yes	Yes
Veber (GSK) filter	No;	Yes
Egan (Pharmacia) filter	No;	Yes
Muegge (Bayer) filter	No;	Yes
£Bioavailability Score	0.55	0.55
Medicinal chemistry		
PAINS	1 alert: dhp_amino_CN_A	1 alert: dhp_amino_CN_A
Brenk	2 alerts: nitro_group; oxygen-nitrogen_single_bond	0 alert
Leadlikeness	No; 1 violation: MW > 350	No; 1 violation: MW > 350
Synthetic accessibility	4.54	4.59

* TPSA: Topological Polar Surface Area. Molecular polar surface area (PSA) calculated as sum of tabulated surface contributions of polar fragments [46].

ESOL – Estimated SOLubility: Simple method for estimating the aqueous solubility of a compound directly from its structure [47]. Soulbility Class: Log S scale:- Insuluble < −10 < Poorly < −6 < Moderately < −4 < Soluble < −2 < Very < 0 < Highly. GI absorption is according to the white of the BIOLED-Egg and BBB permeation is according to the yolk of the BIOLED-Egg.

$ LogKp: Permeability coefficient from the Quantitative Structure Permeability Relationships (QSPR) model based upon permeant size [molecular volume (MV) or molecular weight (MW)] and octanol/water partition coefficient (Koct) [48].

£ Abbott Bioavailability Score: Probability that a compound will have F > 10% in the rat [49].

6.90–7.32 (9H, m); ^{13}C NMR (75 MHz, $CDCl_3$): δ_C 38.9, 46.5, 46.9, 55.9, 56.2, 60.4, 110.5, 111.4, 115.6, 117.4, 120.3, 121.6, 128.7, 129.4, 130.4, 131.3, 141.4, 157.3, 157.8, 159.6. LC/MS (ESI): 401 (M^+). Anal. calcd for $C_{24}H_{23}N_3O_3$: C, 71.80; H, 5.77; N, 10.47%; found: C, 71.67; H, 5.59; N, 10.35%.

4.12. Characterization data for compound **4k**

Light yellow solid, 97% (0.110 g), mp 173–175 °C, IR (KBr)υ_{max} 3328, 2177, 1638, 1601 cm^{-1}; ^{1}H NMR (400 MHz, $CDCl_3$): δ_H 3.12 (1H, d, J = 17.2 Hz), 3.27 (1H, d, J = 17.2 Hz), 3.75 (1H, dd, J = 15.2, 1.6 Hz), 3.88 (1H, dd, J = 15.2, 1.2 Hz), 4.00 (1H, s), 4.73 (2H, s), 6.79 (1H, s), 7.14 (2H, d, J = 8.4 Hz), 7.18 (2H, d, J = 8.4 Hz), 7.32 (2H, d, J = 8.0 Hz), 7.35 (2H, d, J = 7.2 Hz); ^{13}C NMR (100 MHz, $CDCl_3$): δ_C 41.3, 46.3, 46.8, 60.4, 114.9, 120.0, 121.7, 128.2, 129.0, 129.5, 129.6, 130.8, 133.6, 133.9, 134.9, 140.8, 141.1, 159.4. LC/MS (ESI): 411 (M^+). Anal. calcd for $C_{22}H_{17}Cl_2N_3O$: C, 64.40; H, 4.18; N, 10.24%; found: C, 64.61; H, 4.34; N, 10.15%.

4.13. Characterization data for compound **4l**

White solid, 96% (0.110 g), mp 192–196 °C, IR (KBr)υ_{max} 3321, 2177, 1631, 1605 cm^{-1}; ^{1}H NMR (400 MHz, $CDCl_3$): δ_H 3.08 (1H, d, J = 17.2 Hz), 3.26 (1H, d, J = 17.2 Hz), 3.72 (1H, d, J = 15.2 Hz), 3.85 (1H, d, J = 15.2 Hz), 3.97 (1H, s) , 5.91 (2H, s), 6.85 (1H, s), 7.11 (2H, d, J = 8.4 Hz), 7.15 (2H, d, J = 8.4 Hz), 7.45–7.49 (4H, m); ^{13}C NMR (100 MHz, $CDCl_3$): δ_C 40.7, 45.4, 45.9, 57.1, 114.0, 119.9, 120.4, 120.5, 120.6, 128.1, 129.2, 130.3, 131.0, 131.4, 134.9, 139.9, 141.7, 159.4. LC/MS (ESI): 499 (M^+). Anal. calcd for $C_{22}H_{17}Br_2N_3O$: C, 52.93; H, 3.43; N, 8.42%; found: C, 52.83; H, 3.25; N, 8.30%.

4.14. Characterization data for compound **4m**

light yellow solid, 98% (0.118 g), mp 180–182 °C, IR (KBr)υ_{max} 3335, 2177, 1631, 1598 cm^{-1}; ^{1}H NMR (400 MHz, $CDCl_3$): δ_H 3.14 (1H, d, J = 16.8 Hz), 3.28 (1H, d, J = 17.2 Hz), 3.77 (1H, dd, J = 15.2, 1.2 Hz), 3.90 (1H, d, J = 15.2 Hz), 4.01 (1H, s), 4.73 (2H, s), 6.82 (1H, s), 7.02–7.25 (8H, m); ^{13}C NMR (100 MHz, $CDCl_3$): δ_C 41.1, 46.3, 46.8, 60.7, 114.8, 115.8 (d, J = 21.4 Hz), 116.3 (d, J = 21.5 Hz), 120.0, 121.7, 127.7, 129.8 (d, J = 8.2 Hz), 131.2 (d, J = 8.1 Hz), 132.8, 135.3, 140.7, 159.3, 162.4, 162.6. LC/MS (ESI): 377 (M^+). Anal. calcd for $C_{22}H_{17}F_2N_3O$: C, 70.02; H, 4.54; N, 11.13%; found: C, 70.30; H, 4.40; N, 11.22%.

4.15. Characterization data for compound **4n**

Yellow solid, 97% (0.114 g), mp 202–205 °C, IR (KBr)υ_{max} 3306, 2191, 1642, 1598 cm^{-1}; ^{1}H NMR (400 MHz, $CDCl_3$): δ_H 2.94 (1H, d, J = 17.2 Hz), 3.24 (1H, d, J = 17.6 Hz), 3.59 (1H, d, J = 15.6 Hz), 3.69 (1H, d, J = 15.6 Hz), 4.85 (1H, s), 5.22 (2H, s), 7.21 (1H, d, J = 6.8 Hz), 7.37–7.53 (8H, m), 7.74–7.87 (4H, m), 8.03 (1H, d, J = 8.8 Hz), 8.19 (1H, d, J = 8.4 Hz); ^{13}C NMR (100 MHz, $CDCl_3$): δ_C 40.2, 46.6, 47.0, 59.8, 115.8, 120.3, 120.5, 123.1, 125.2, 125.4, 125.6, 126.1, 126.4, 126.6, 126.7, 127.1, 127.2, 127.8, 128.3, 128.9, 129.4, 129.9, 131.9, 132.3, 133.5, 133.9, 134.5, 137.1, 140.9, 160.1. LC/MS (ESI): 441 (M^+). Anal. calcd for $C_{30}H_{23}N_3O$: C, 81.61; H, 5.25; N, 9.52%; found: C, 81.83; H, 5.39; N, 9.40%.

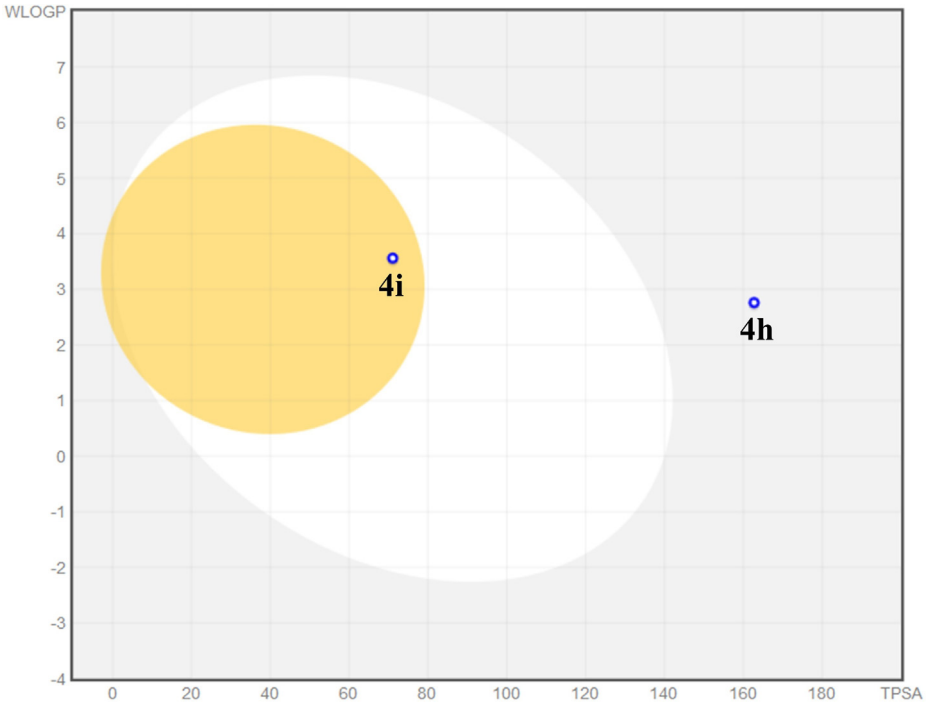

Fig. 8. BOILED-Egg representation of compounds **4h** and **4i.**

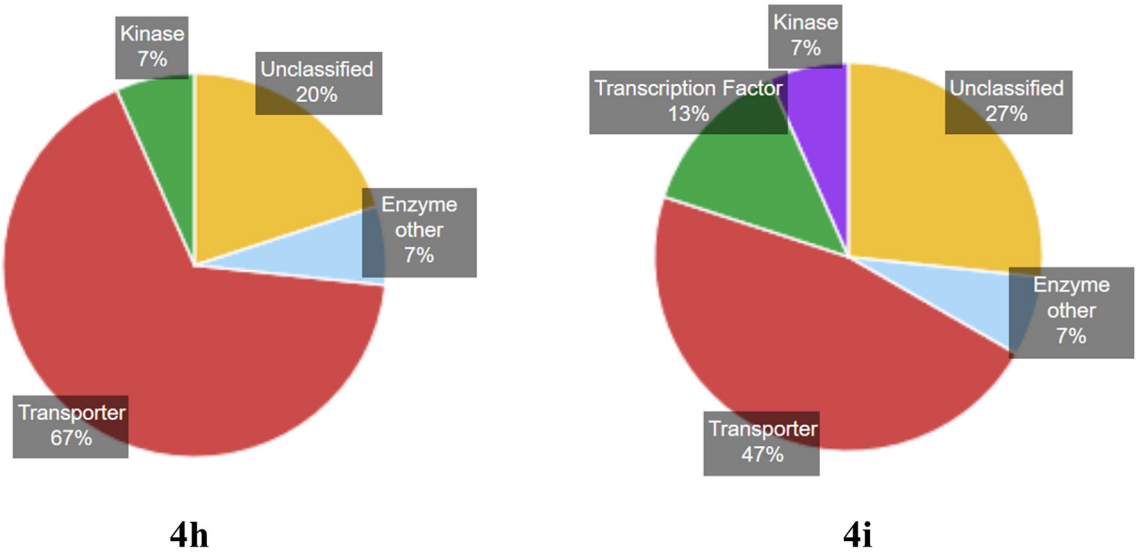

Fig. 9. Predicted target classes of the compounds **4h** and **4i.**

Acknowledgements

The authors thank the Deanship of Scientific Research at King Saud University for funding this work through research group No. RG-1438-052.

References

[1] R.N. Kalaria, G.E. Maestre, R. Arizaga, R.P. Friedland, D. Galasko, K. Hall, J.A. Luchsinger, A. Ogunniyi, E.K. Perry, F. Potocnik, M. Prince, R. Stewart, A. Wimo, Z.X. Zhang, P. Antuono, Lancet Neurol. 7 (2008) 812.
[2] S. Salloway, S. Correia, Cleve. Clin. J. Med. 76 (2009) 49.
[3] D.J. Selkoe, Ann. Intern. Med. 140 (2004) 627.
[4] I. Yanovsky, E. Finkin-Groner, A. Zaikin, L. Lerman, H. Shalom, S. Zeeli, T. Weill, I. Ginsburg, A. Nudelman, M. Weinstock, J. Med. Chem. 55 (2012) 10700.
[5] D. Munoz-Torrero, Curr. Med. Chem. 15 (2008) 2433.
[6] R.S. Kumar, A.I. Almansour, N. Arumugam, D.M. Al-thamili, M. Altaf, A. Basiri, D. Kotresha, T.S. Manohar, S. Venketesh, Bioorg. Chem. 77 (2018) 263.
[7] A. Basiri, B.M. Abd Razik, M.O. Ezzat, Y. Kia, R.S. Kumar, A.I. Almansour, N. Arumugam, V. Murugaiyah, Bioorg. Chem. 75 (2017) 210.
[8] R.S. Kumar, A.I. Almansour, N. Arumugam, A. Basiri, Y. Kia, R.R. Kumar, Aust. J. Chem. 68 (2015) 863.
[9] A.I. Almansour, R.S. Kumar, N. Arumugam, A. Basiri, Y. Kia, M.A. Ali, M. Farooq, V. Murugaiyah, Molecules 20 (2015) 2296.
[10] A.I. Almansour, R.S. Kumar, N. Arumugam, A. Basiri, Y. Kia, M.A. Ali, BioMed. Res. Int. 965987 (2015) 1.
[11] Y. Kia, H. Osman, R.S. Kumar, A. Basiri, V. Murugaiyah, Bioorg. Med. Chem. Lett. 24 (2014) 1815.
[12] Y. Kia, H. Osman, R.S. Kumar, A. Basiri, V. Murugaiyah, Bioorg. Med. Chem. 22 (2014) 1318.
[13] A. Basiri, V. Murugaiyah, H. Osman, R.S. Kumar, Y. Kia, M.A. Ali, Bioorg. Med. Chem. 21 (2013) 3022.
[14] A. Basiri, V. Murugaiyah, H. Osman, R.S. Kumar, Y. Kia, K.B. Awang, M.A. Ali, Eur. J. Med. Chem. 67 (2013) 221.
[15] M.A. Ali, R. Ismail, T.S. Choon, R.S. Kumar, M. Asad, A.I. Almansour, Y.K. Yoon, A.C. Wei, K. Elumalai, S. Pandian, Med. Chem. 2 (2012) 7.
[16] A.M. El-Agrody, M.S. Abd El-Latif, N.A. El-Hady, A.H. Fakery, A.H. Bedair,

Molecule 6 (2001) 519.
[17] A.M. El-Agrody, M.H. El-Hakim, M.S. Abd El-Latif, A.H. Fakery, E.M. El-Sayed, K.A. El-Ghareab, Acta Pharm. 50 (2000) 111.
[18] M. Perez-Perez, J. Balzarini, J. Rozenski, E. De Clercq, P. Herdewijn, Bioorg. Med. Chem. Lett. 5 (1995) 1115.
[19] A.H. Shamroukh, M.E.A. Zaki, E.M.H. Morsy, F.M. Abdel-Motti, F.M.E. Abdel-Megeid, Arch. Pharm. 340 (2007) 236.
[20] M.D. Aytemir, U. Calis, M. Ozalp, Arch. Pharm. 337 (2004) 281.
[21] E. Melliou, P. Magiatis, S. Mitaku, A.L. Skaltsounis, A. Pierre, G. Atassi, P. Renard, Bioorg. Med. Chem. 9 (2001) 607.
[22] F. Chabchoub, M. Messaad, H.B. Mansour, L. Chekir-Ghedira, M. Salem, Eur. J. Med. Chem. 42 (2007) 715.
[23] S. Hatakeyama, N. Ochi, H. Numata, S. Takano, J. Chem. Soc., Chem. Commun. 17 (1988) 1202.
[24] K. Singh, J. Singh, H. Singh, Tetrahedron 52 (1996) 14273.
[25] N. Martin, A. Martinez-Grau, C. Seoane, J.L. Marco, A. Albert, F.H. Cano, Liebigs Ann. Chem. 7 (1993) 801.
[26] A. Martinez-Grau, J.L. Marco, Bioorg. Med. Chem. Lett. 7 (1997) 3165.
[27] L. Bonsignore, G. Loy, D. Secci, A. Calignano, Eur. J. Med. Chem. 28 (1993) 517.
[28] D. Kumar, V.B. Reddy, S. Sharad, U. Dube, S. Kapur, Eur. J. Med. Chem. 44 (2009) 3805.
[29] J.L. Wang, D. Liu, Z.J. Zheng, S. Shan, X. Han, S.M. Srinivasula, C.M. Croce, E.S. Alnemri, Z. Huang, Proc. Natl. Acad. Sci. U. S. A. 97 (2000) 7124.
[30] C.S. Konkoy, D.B. Fick, S.X. Cai, N.C. Lan, J.F. Keana, W. Int. Appl. WO 00/75123 A1, 2000 transChem. Abstr. 2001, 134, 29313a.
[31] D. Shi, J. Mou, Q. Zhuang, X. Wang, J. Chem. Res. (2004) 821.
[32] R.H. Poyser, T.C. Hamilton, Drugs Fut. 19 (1994) 39.
[33] J.R. Empfield, K. Russell, Annu. Rep. Med. Chem. 30 (1996) 81.
[34] B. Pirotte, J. Fontaine, P. Lebrun, Curr. Med. Chem. 2 (1995) 573.
[35] K.S. Atwal, Curr. Med. Chem. 3 (1996) 227.
[36] W. Kemnitzer, J. Drewe, S. Jiang, H. Zhang, Y. Wang, J. Zhao, S. Jia, J. Herich, D. Labreque, R. Storer, K. Meerovitch, D. Bouffard, R. Rej, R. Denis, C. Blais, S. Lamothe, G. Attardo, H. Gourdeau, B. Tseng, S. Kasibhatla, S.X. Cai, J. Med. Chem. 47 (2004) 6299.
[37] S.A. Patil, R. Patil, L.M. Pfeffer, D.D. Miller, Future, Med. Chem. 5 (2013) 1647.
[38] K.A. Birch, W.F. Heath, R.N. Hermeling, C.M. Johnston, L. Stramm, C. Dell, Diabetes 45 (1996) 642.
[39] C. Wiener, C.H. Schroeder, B.D. West, K.P. Link, J. Org. Chem. 27 (1962) 3086.
[40] C.W. Smith, J.M. Bailey, M.E. Billingham, S. Chandrasekhar, C.P. Dell, A.K. Harvey, Bioorg. Med. Chem. Lett. 5 (1995) 2783.
[41] C.S. Konkoy, D.B. Fick, S.X. Cai, N.C. Lan, J.F.W. Keana, PCT Int Appl. 134 (2000) 2931a WO0075123; Chem. Abstr..
[42] J.R. Dimmock, M.P. Padmanilayam, R.N. Puthucode, A.J. Nazarali, N.L. Motaganahalli, G.A. Zello, J.W. Quail, E.O. Oloo, H.-B. Kraatz, J.S. Prisciak, T.M. Allen, C.L. Santos, J. Balzarini, E. De Clercq, E.K. Manavathu, J. Med. Chem. 44 (2001) 586.
[43] N. Arumugam, A.I. Almansour, R.S. Kumar, M. Altaf, R. Padmanaban, P. Sureshbabu, G. Angamuthu, D. Kotresha, T.S. Manohar, S. Venketesh, Bioorg. Chem. 79 (2018) 64.
[44] Antoine Daina, O. Michielin, V. Zoete, Sci. Rep. 7 (2017) 42717.
[45] Antoine Daina, V. Zoete, Chem. Med. Chem. 11.11 (2016) 1117.
[46] P. Ertl, B. Rohde, P. Selzer, J. Med. Chem. 43 (2000) 3714.
[47] J.S. Delaney, J. Chem. Inf. Comput. Sci. 44 (2004) 1000.
[48] R.O. Potts, R.H. Guy, Pharm. Res. 9 (1992) 663.
[49] Y.C. Martin, J. Med. Chem. 48 (2005) 3164.
[50] D. Gfeller, O. Michielin, V. Zoete, Bioinformatics 29 (2013) 3073.